

Numerical study of hydrofoil tip vortex fluid field

PU Jijun, XIONG Ying

Department of Naval Architecture Engineering, Naval University of Engineering, Wuhan 430033, China

Abstract: Three different models, $k-\omega$, DES and LES, are conducted in the analysis of the tip vortex flow field. In order to reduce the discrete error induced by the grid, mesh refinement is applied to the area of the tip vortex core in numerical simulations. The axis and tangential velocities of the tip vortex flow field with no cavitation are calculated, and the calculated velocities agree well with the experimental results. On the basis of this process, the influence of vortex roll-up on the tip vortex pressure field is discussed, and bubble static equilibrium is proposed by which the tip vortex cavitation inception number is computed.

Key words: tip vortex; bubble static equilibrium; cavitation inception; hydrofoil

CLC number: U661.313

0 Introduction

Since the early research of Besant^[1] in 1859, tip vortex cavitation has been the focus of scholars. When a gas nucleus enters the vortex nucleus, if the pressure is smaller than the critical pressure, the gas nucleus will grow rapidly and form a macroscopic cavitation. The cavitation will release strong radiation noise and cause denudation of propeller and rudder in the collapse process. The types of cavitation include tip vortex cavitation, sheet cavitation, cloud cavitation and wandering cavitation. A lot of experiments have shown that the local pressure at the center of the tip vortex core is the minimum, and except the unloaded 3D hydrofoils and propellers at the tip, tip vortex cavitation appeared first among all types of cavitation (Keller^[2] has found this in the related experiments). The noise it produces will have a huge impact on the ship stealth. In order to suppress the generation of tip vortex cavitation, it is necessary to calculate the flow field characteristics of the tip vortex accurately. However, due to the instability of tip vortex itself, it is still a difficult problem to accurately grasp the characteristics of tip vortex flow field. The effective way to solve this problem is to carry out the high accuracy numerical calculation, which can

provide specific details of the tip vortex flow field.

Fruman and Arndt et al.^[3-4] have carried out a large number of studies on the flow field distribution of tip vortex. Compared with experiments, numerical calculation has high efficiency and low cost, and it is easier to obtain the details of flow field distribution of tip vortex. Therefore, it has increasingly been the mainstream to use numerical methods to calculate the tip vortex flow field. But it is worth noting that the velocity gradient of the tip vortex flow field is large and the distribution of flow field is complex. It is necessary to select appropriate turbulence model and refine the meshes of the tip vortex flow field. At present, the widely used RANS method averages the Reynolds term, which can only obtain the time-averaged turbulence results, and ignores the small-scale change of the turbulence structure, making the effect of RANS in the tip vortex simulation not ideal^[5]. In the aspect of computational grid, Turnock et al.^[6] proposed a method to locate the tip vortex trajectory by finding the lowest point of pressure, and the computational accuracy was greatly improved by this method. Zhang et al.^[7] believed that the computational accuracy can only be satisfied when the number of the radial mesh nodes of the vortex core should be greater than 15 in the numerical calculation.

Received: 2016 - 06 - 03

Supported by: National Natural Science Foundation of China (51179198)

Author(s): PU Jijun, male, born in 1991, master candidate. Research interest: fluid mechanics. E-mail: 211982361@qq.com

XIONG Ying (Corresponding author), male, born in 1958, Ph. D., professor, doctoral supervisor. Research interest: ship fluid mechanics. E-mail: ying_xiong28@126.com

In this paper, the numerical model is a semi-elliptical hydrofoil with a profile of NACA 16020 wing shape, and the flow field distribution is calculated by using different turbulence models, which are compared with the experimental results so as to select the suitable vortex model. On this basis, the number of tip vortex cavitation inception is calculated by using the bubble static equation.

1 Numerical method

1.1 Introduction of RANS model

RANS model is a kind of turbulence model which can carry out time-averaged process on the fluid mass, momentum and so on^[8]. The Reynolds average method does not need to calculate the turbulent flow at different scales, but only the mean motion. When the turbulence structure of fluid is more complex, the RANS model can only give the time-averaged results. Therefore, the RANS model is not suitable for complex flow phenomena.

The Reynolds averaged N-S equation is shown as below:

$$\frac{\partial \rho u_i}{\partial t} + \frac{\partial \rho u_i u_j}{\partial x_j} = -f_i - \frac{\partial p}{\partial x_j} + \frac{\partial}{\partial x_j} \left[u \left(\frac{\partial u_i}{\partial x_j} + \frac{\partial u_j}{\partial x_i} - \frac{2}{3} \delta_{ij} \frac{\partial u_l}{\partial x_l} \right) \right] + \frac{\partial \rho}{\partial x_j} (-\overline{\rho u_i u_j}) \quad (1)$$

where $x_i (i=1, 2, 3)$, $x_j (j=1, 2, 3)$, and $x_l (l=1, 2, 3)$ are the direction coordinates in the three-dimensional Cartesian coordinate system; t is the time; u_i , u_j and u_l are the velocity components; ρ is fluid density; u is dynamic viscosity coefficient; $\tau_{ij} = -\overline{\rho u_i u_j}$ is Reynolds stress; f_i is volume force; and $\delta_{ij} = \begin{cases} 1, & i=j \\ 0, & i \neq j \end{cases}$.

1.2 Introduction of LES model

There are turbulence structures at various scales in turbulent flow, and the large scale vortex is mainly the turbulent structure with the size larger than the mean flow (note: shear layer thickness). Compared with large scale vortex, small scale vortex mainly plays the role of dissipation of turbulent energy. Based on the basic phenomenon, the LES method calculates the large scale vortex with the direct numerical solution method and solves small scale vortex through establishing model. The boundary scale that separates the large and small scale vortices in the model is called the filtering scale, represented by Δ . Compared with the ordinary RANS model, it re-

quires more detailed grid distribution and more computing resources^[9].

The governing equation of LES is as follows:

$$\frac{\partial \overline{u}_i}{\partial t} + \frac{\partial \overline{u}_i \overline{u}_j}{x_j} = -\frac{1}{\rho} \frac{\partial \overline{p}}{\partial x_i} + \nu \frac{\partial^2 \overline{u}_i}{\partial x_i \partial x_j} + \frac{\partial \overline{\tau}_{ij}}{\partial x_j} \quad (2)$$

where \overline{p} is average pressure; $\overline{\tau}_{ij} = (\overline{u_i u_j} - \overline{u_i} \overline{u_j})$ is a sub-grid stress, meaning the energy dissipation and transmission between small scale turbulent fluctuation after filtering and large scale vortex. The representation of sub-grid stress is as follows:

$$\overline{\tau}_{ij} = L_{ij} + C_{ij} + R_{ij} \quad (3)$$

where L_{ij} is Leonard stress, which represents the interaction between the large scale vortices; C_{ij} is interaction stress, which represents the interaction between large scale and small scale vortices; R_{ij} is sub-grid Reynolds stress, which represents the interaction between the small scale vortices^[10]. L_{ij} , C_{ij} and R_{ij} are represented as follows:

$$L_{ij} = (\overline{u_i u_j} - \overline{\overline{u_i} \overline{u_j}}) \quad (4)$$

$$C_{ij} = (\overline{u_i u_j} - \overline{\overline{u_i} \overline{u_j}}) \quad (5)$$

$$R_{ij} = -\overline{u_i'' u_j''} \quad (6)$$

1.3 Introduction of DES model

DES model is a kind of turbulence model between RANS and LES. It uses the RANS model in the boundary layer, and the LES model in other areas. It occupies more computing resources than the RANS model, but fewer than the LES model. The DES studied in this paper is $k-\omega$ based turbulence model.

Compared with the $k-\omega$ model, the DES model proposed the modification of dissipation term Y_k in this paper as follows:

$$Y_k = \rho \beta^* k \omega F \quad (7)$$

where $F = \max\left(\frac{L_t}{C \Delta_{\max}}, 1\right)$, and C is a calibration constant in the DES model, the default value is 0.61, Δ_{\max} is the local maximum grid distance, $L_t = \frac{\sqrt{k}}{\beta^* \omega}$, β^* is an uncertain parameter.

2 Computational model and mesh

In this paper, the computational model is a semi-elliptical hydrofoil with a profile of NACA 16020 wing shape. The experiment^[3] has been completed in the cavitation water tunnel, with the inflow velocity of 10 m/s and the wing angle of attack of 10°. The entrance 3 times the length of chord away from the hydrofoil is set as the velocity entrance; the

outlet 10 times the length of chord away from the hydrofoil is set as the pressure outlet. The origin is located at the center of the root of the hydrofoil. The computational domain is shown in Fig. 1.

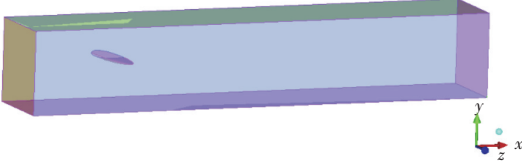


Fig.1 Computational domain

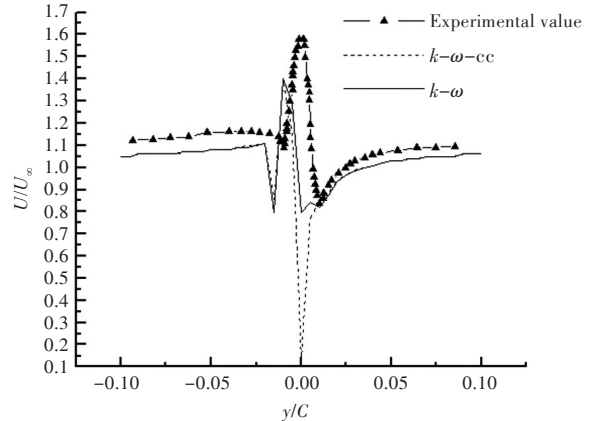
According to the geometry of the computational domain, this paper mainly uses the H grid for the overall meshing of the computational domain. Considering that the formation of tip vortex is related to flow in the wing boundary layer, to accurately simulate the flow field in the boundary layer, we used O grid to deal with the meshes near the wing's wall, so as to improve the quality of the grid. Scale y^+ of the first layer of grid is 1–30. To compare with the experimental results, the computational domain established in this paper is consistent with the experimental results. We construct 2 coordinate systems in this paper, of which the origin of the absolute coordinates is located at the center of the chord of hydrofoil bottom, and the directions of x , y , and z are shown in Fig. 1. In order to facilitate the analysis of the tip vortex, the relative coordinate system is set up in this paper, and its origin is located at the center of the tip vortex core at each interface, with the directions of x , y , and z being the same as those of the absolute coordinate system. When not explicitly shown, the default is the absolute coordinate system.

According to the method of Turnock et al.^[6], through the preliminary calculation, positions of the points with the lowest pressure of each section in the wake flow area were obtained, and connection of these points can be considered as the tip vortex trajectory. The radial and axial mesh refinement was conducted to the line, so as to obtain the optimized meshes. At the same time, Dehghan et al.^[8] also pointed out that, in the numerical calculation, the number of the radial mesh nodes of the vortex core should be greater than 15 to meet the calculation accuracy. The mesh nodes in the vortex core are divided as 20×20 , and the total mesh number is 8 million.

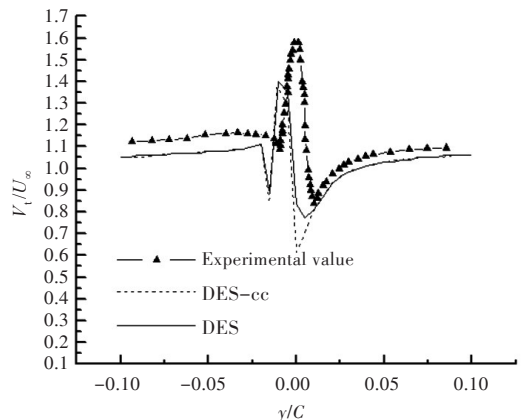
3 Numerical study of tip vortex flow field

Tip vortex flow field of 3D hydrofoil has complex structure, and the influence of mutual interference

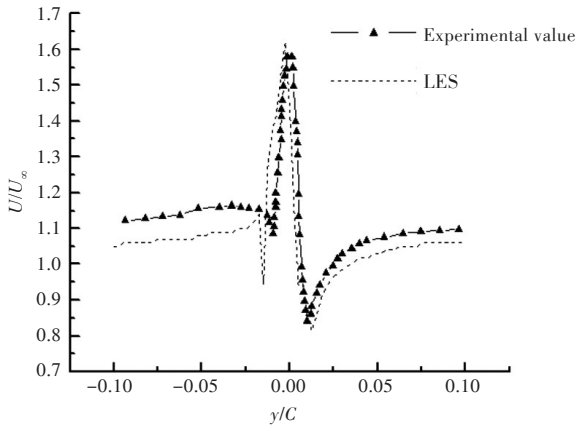
between the main vortex and the secondary vortex brings considerable difficulty to the numerical simulation. At the same time, energy dissipation of tip vortex also makes it difficult to use the turbulence model. In the application of different turbulence models, there is a big difference between the axial velocity and the experimental value. Spalart et al.^[11] pointed out that the turbulence model after rotation and curvature modification, can effectively restrain the viscous dissipation at the vortex core, thus improving the computational accuracy. However, it is found that the turbulence model with modified curvature can reduce the axial velocity of the tip vortex reversely, which makes it more different from the experimental results. Figs. 2 and 3 give the calculated results and experimental results of the dimensionless axial velocity (U/U_∞) and the tangential velocity (V_t/U_∞) of tip vortex flow field distributed along the y axis of 3 positions in the x direction. Among them, the axial direction refers to the direction parallel with the tip vortex line, and tangential direction is the direction vertical to the tip vortex line. Due to that the tip vortex trajectory is approximately parallel to the x axis direction (the inflow direction), here axial velocity is



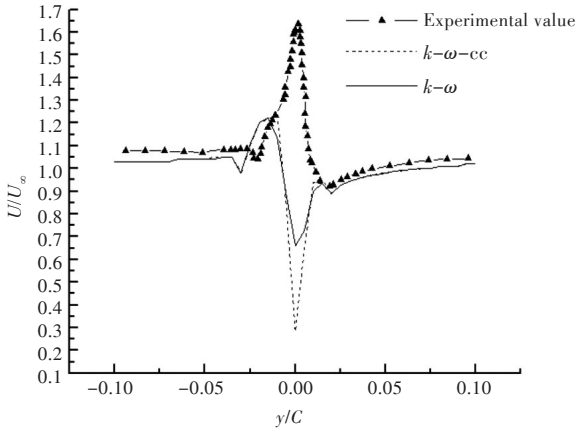
(a) Comparison between the calculated value and experimental value of $k-\omega$ model when $x/C=0.1$



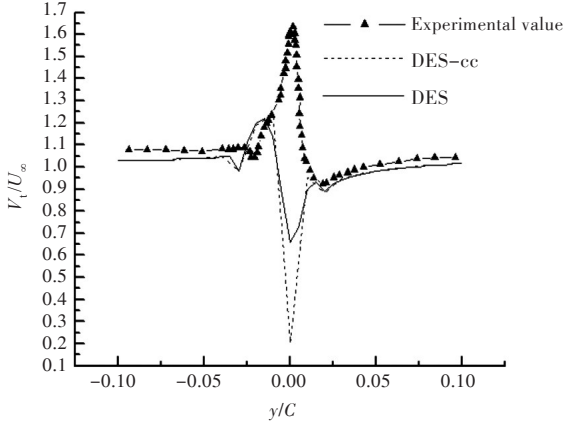
(b) Comparison between the calculated value and experimental value of DES model when $x/C=0.1$



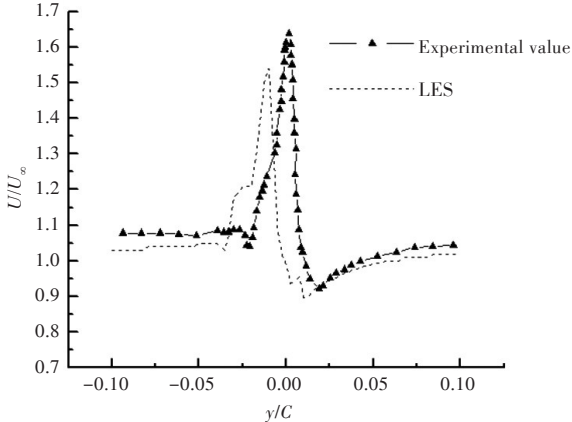
(c) Comparison between the calculated value and experimental value of LES model when $x/C=0.1$



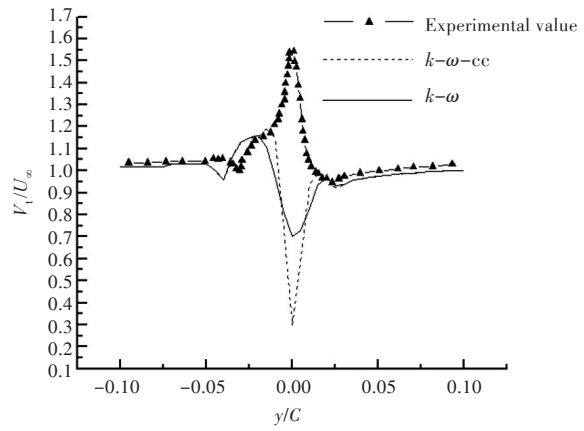
(d) Comparison between the calculated value and experimental value of $k-\omega$ model when $x/C=0.2$



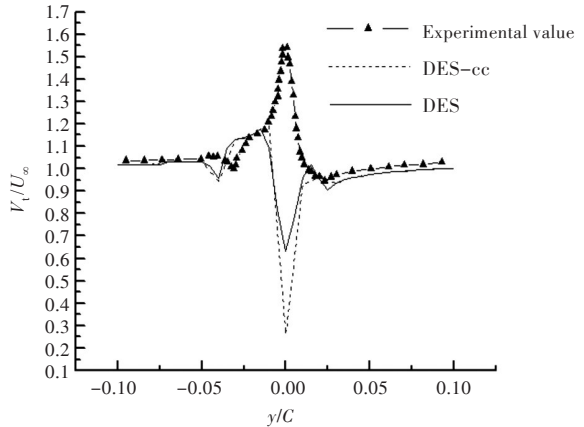
(e) Comparison between the calculated value and experimental value of DES model when $x/C=0.2$



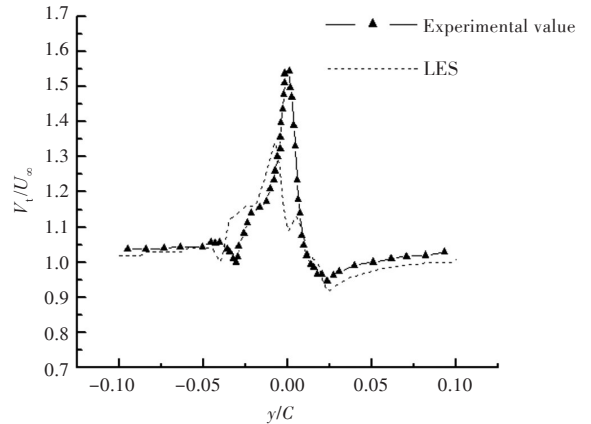
(f) Comparison between the calculated value and experimental value of LES model when $x/C=0.2$



(g) Comparison between the calculated value and experimental value of $k-\omega$ model when $x/C=0.3$



(h) Comparison between the calculated value and experimental value of DES model when $x/C=0.3$



(i) Comparison between the calculated value and experimental value of LES model when $x/C=0.3$

Fig.2 Profiles of axial velocity in tip vortex

considered x direction velocity, and the tangential velocity is z direction velocity.

As can be seen from Fig. 2, the $k-\omega$ model and the $k-\omega$ based DES model have a large error in predicting the axial velocity of the tip vortex. Especially, the velocity distribution at the vortex core is opposite to the experimental values. It is possible that the two models have overly predicted the viscous dissipation of the tip vortex, which makes the velocity drop

too fast. Using the turbulence model of modified curvature still further increases the viscous dissipation, which is obviously different from the conclusions of Reference [10]. The possible reason is that the use of curvature correction is based on some prerequisite conditions, otherwise we will get the opposite conclusion, and research on curvature correction will be further carried out in the future. The LES turbulence model gives good prediction results, and especially, the velocity distribution of the vortex core at $x/C = 0.1$ is in good agreement with the experimental values. While in the observation of tip vortex cavitation, it was found that the tip vortex cavitation inception position was generally near $x/C = 0.1$. Therefore, the accurate simulation of the velocity flow field at this position lays a good foundation for the further study of the tip vortex cavitation inception.

It can be seen from Fig. 3 that the prediction effect of each turbulence model on the tangential velocity distribution of the tip vortex is good. Especially in the case of $x/C = 0.3$ of LES model, when the tip vortex viscosity has larger dissipation, it can be still in good agreement with the experimental values. However, there is a small error between the predicted results of each turbulence model and the experimental values in the area of local coordinates $z < 0$, which

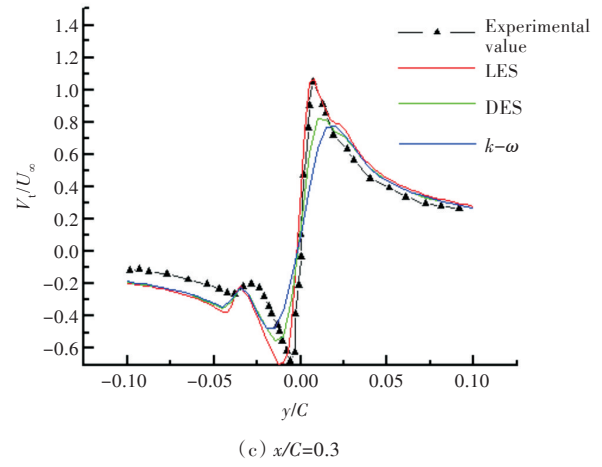
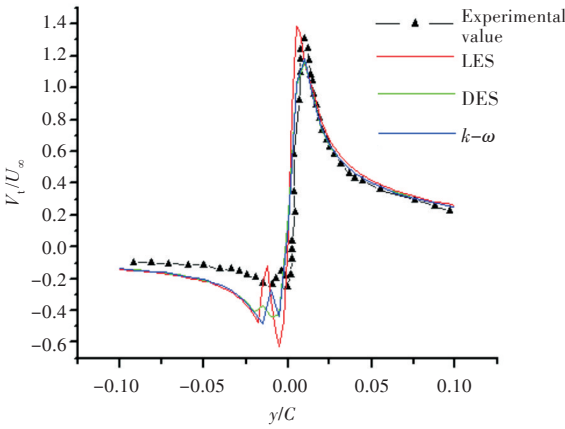
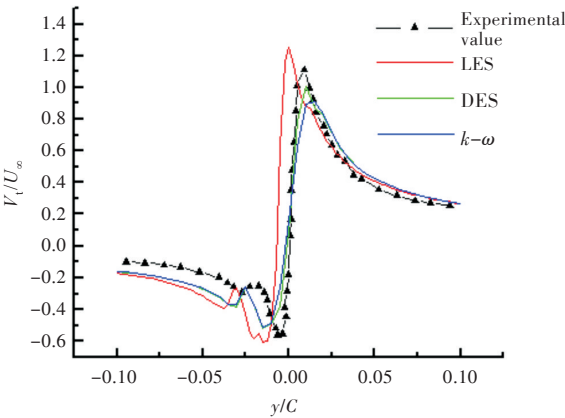


Fig.3 Profiles of tangential velocity in tip vortex

may be due to the interference of the three-dimensional hydrofoil wall on the main vortex. Fig. 4 shows the minimum pressure coefficient distribution (C_p) at the vortex core along the x direction, and the minimum pressures of LES, DES and RANS models are all at $x/C = 0.355$, corresponding to the minimum pressure coefficients of -7.38 , -7.05 and -5.98 , respectively. It is obvious that the RANS turbulence model overly predicted the viscous dissipation, which makes the minimum pressure coefficients have larger difference with the LES and DES prediction results. As can be obviously seen from Fig. 4, the minimum pressure coefficient curves given in the LES and DES turbulence models have a more obvious secondary reduction area. The existence of this area is because when the main vortex moves along the tip vortex trajectory direction, other wake vortices generated by hydrofoils will be rolled in, and when the two vortices twine and merge in screw type, the main vortex strength will increase, so that the flow velocity in the vortex core increases and the pressure is reduced. At the same time, energy will continue to dissipate in the motion process of the



(a) $x/C=0.1$



(b) $x/C=0.2$

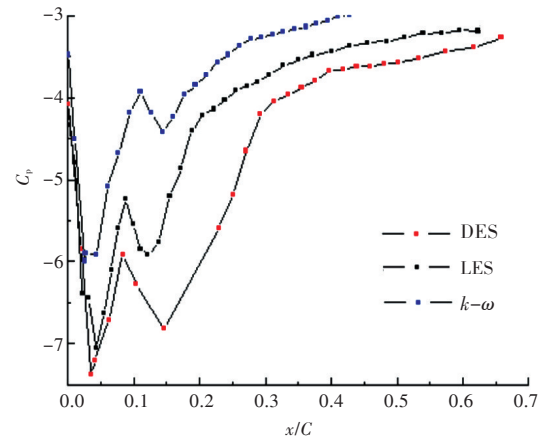


Fig.4 Pressure coefficients along the tip vortex trajectory

main vortex, so there is a relatively balanced point to make the main vortex's dissipated energy dissipation equal the roll-up energy.

4 Bubble static equilibrium and calculation of the number of tip vortex cavitation inception

The classical Rayleigh–Plesset equation used to describe the variation of microbubble volume is

$$R_b \frac{d^2 R_b}{dt^2} + \frac{3}{2} \left(\frac{dR_b}{dt} \right)^2 + \frac{4\nu}{R_b} \frac{dR_b}{dt} = \frac{1}{\rho} \left(p_v + p_{g0} \left(\frac{R_0}{R_b} \right)^{3k} - p_{\text{encouter}} - \frac{2S}{R_b} \right) + \frac{(U - U_b)^2}{4} \quad (8)$$

The left side of the equation is a dynamic term, which represents the change of the volume of bubble; the right side is a static term, which is only related with the force of bubble. When the bubble volume changes relatively slowly, the dynamic term on the left side of the equation can be neglected, and the equation is simplified as the static equilibrium equation during the study of cavitation inception:

$$P_e - P_v = P_g - \frac{2S}{R_b} \quad (9)$$

In Eq. (8) and (9): P_e is ambient pressure around a bubble, and when the bubble volume is very small, P_e is usually set to the pressure of the center point of the bubble; P_v is the saturated vapor pressure; P_g is the gas pressure in the bubble; R_b is bubble radius; S is the tension coefficient of bubble surface; R_0 is the initial bubble radius; ν is kinematic viscosity coefficient; p_v and p_{encouter} are pressures around the bubble; U is fluid velocity; U_b is bubble velocity; p_{g0} is the gas pressure inside the initial bubble.

When the ambient pressure changes around a bubble, the radius of the bubble will change according to its equilibrium state. Because the velocity of liquid gasification is very fast when cavitation happens, the vapor pressure in the bubble is set to constant. On the other hand, the velocity of gas diffusion in water is very slow compared with the velocity of cavitation, so it can be assumed that the mass of gas in bubble is constant. So the expression of P_g is as follows:

$$P_g = P_{g0} \left(\frac{R_0}{R_b} \right)^2 \quad (10)$$

The final bubble equilibrium equation is

$$P_e - P_v = P_{g0} \left(\frac{R_0}{R_b} \right)^2 - \frac{2S}{R_b} \quad (11)$$

where

$$P_{g0} = P_0 - P_v + \frac{2S}{R_0} \quad (12)$$

Fig. 5 shows the static equilibrium curves of spherical bubbles^[12], where Critical values represent the critical boundary line. The area below the boundary line belongs to the non-equilibrium area, and the bubbles in the area will grow rapidly. Therefore, the critical pressure and critical radius can be determined by the intersection of the boundary line and the static equilibrium curves.

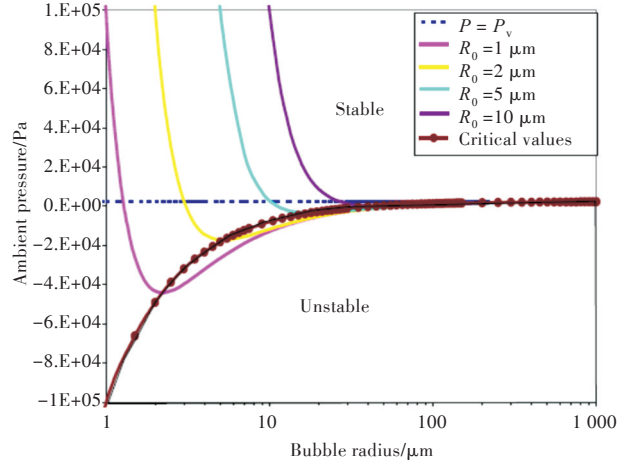


Fig.5 Static equilibrium curves of bubbles^[12]

The critical pressure P_c and critical radius R_c obtained are as follows:

$$P_c = P_v - \frac{4S}{3R_c} \quad (13)$$

$$R_c = \left[\frac{3R_0^3}{2S} \left(P_0 - P_v + \frac{2S}{R_0} \right) \right]^{\frac{1}{2}} \quad (14)$$

When the pressure in the flow field is less than the critical pressure P_c , the bubble will grow rapidly, and the tip vortex cavitation will appear accordingly. When the bubble equilibrium equation is used, not only the flow field environment is considered, but also the initial radius of the gas core needs to be considered. The initial bubble radii R_0 are set as 30, 50, 100 μm , and P_v is 3 540 Pa, so as to investigate the number of tip vortex cavitation at different initial radii.

It is known that the minimum pressure coefficient of a three-dimensional hydrofoil is -7.38 (the result calculated through the LES model). During the tip vortex cavitation inception, $P_e = P_c$. Eq. (13) and (14) are simultaneous, then R_c , P_c and the number δ_i of cavitation inception can be calculated, and the computational results are shown in Table 1.

From the above results, it can be seen that the dif-

Table 1 The computational results of hydrofoil vortex cavitation inception

	$R_0/\mu\text{m}$		
	30	50	100
$R_c/\mu\text{m}$	61.9	122	316
P_c/Pa	-1.5×10^5	-7.5×10^4	2.7×10^4
P_0/Pa	2.16×10^5	2.93×10^5	3.42×10^5
δ_i	4.27	5.81	6.77

ference of critical pressure is large under different initial radii, which leads to the large difference of the number of tip vortex cavitation inception under different initial radii. From the above results, it also can be found that the critical pressure is always less than the vapor pressure, so when the requirement of controlling the tip vortex cavitation inception is higher, the relatively safer vapor pressure can be used to calculate the number of tip vortex cavitation inception. However, when the number of tip vortex cavitation inception needs to be calculated accurately, the critical pressure must be used to calculate the number of tip vortex cavitation inception.

The number of tip vortex cavitation inception can be calculated accurately by using the bubble static equation, which lays the foundation for the study of the scale effect of the number of tip vortex cavitation inception.

5 Conclusions

The $k-\omega$, DES and LES models are used respectively to calculate the tip vortex flow field distribution of elliptical hydrofoil with wing section of NACA 16020 wing. The bubble static equilibrium equation is introduced and combined to study the tip vortex cavitation inception of the hydrofoil, and the following conclusions are obtained:

1) The RANS turbulence model overly predicts the viscous dissipation of the tip vortex, and the results are not improved after using curvature correction, but the axial velocity is reduced reversely, which is opposite to the conclusion of Reference [10]. Better results can be obtained by using LES turbulence model.

2) The LES turbulence model can be used to accurately predict the effect of the roll-up vortex on the pressure field of the tip vortex, which lays the foundation for the subsequent study of the tip vortex cavitation.

3) In the case of using the bubble static equilibrium equation to predict the number of tip vortex cavitation inception, when the requirement of controlling tip vortex cavitation inception is higher, the relative-

ly safer vapor pressure can be used to calculate the number of tip vortex cavitation inception. When the number of the tip vortex cavitation inception needs to be calculated accurately, the critical pressure must be used for calculation.

References

- [1] BESANT W H. A treatise on hydrostatics and hydrodynamics[M]. London: Deighton, Bell, 1859.
- [2] KELLER A P. Cavitation scale effects—empirically found relations and the correlation of cavitation number and hydrodynamic coefficients[C]//CAV 2001: Fourth International Symposium on Cavitation. Pasadena, CA, USA: California Institute of Technology, 2001.
- [3] FRUMAN D H, DUGUÉ C, PAUCHET A, et al. Tip vortex roll-up and cavitation [C]//Proceedings of the 19th Symposium on Naval Hydrodynamics. Washington D C, USA: National Academy, 1992: 633–654.
- [4] ARNDT R E A, ARAKERI V H, HIGUCHI H. Some observations of tip-vortex cavitation[J]. Journal of Fluid Mechanics, 1991, 229: 269–289.
- [5] WU Q, YE Q, MENG G X. Application and comparison of the different turbulent models simulation for non-contact vortex gripper[J]. Journal of Shanghai Jiaotong University, 2013, 47(3): 423–427 (in Chinese).
- [6] TURNOCK S R, PASHIAS C, ROGERS E. Flow feature identification for capture of propeller tip vortex evolution [C]//Proceedings of the 26th Symposium on Naval Hydrodynamics. Rome, Italy: Italian Ship Model Basin, Office of Naval Research, 2006.
- [7] ZHANG L X, ZHANG N, PENG X X, et al. A review of studies of mechanism and prediction of tip vortex cavitation inception [J]. Journal of Hydrodynamics: Ser. B, 2015, 27(4): 488–495.
- [8] DEHGHAN M, TABRIZI H B. Turbulence effects on the granular model of particle motion in a boundary layer flow [J]. The Canadian Journal of Chemical Engineering, 2014, 92(1): 189–195.
- [9] GAN W B, ZHOU Z, XU X P, et al. Investigation on improving the capability of predicting separation in modified SST turbulence model [J]. Journal of Propulsion Technology, 2013, 34(5): 595–602 (in Chinese).
- [10] MORGUT M, NOBILE E, BILUŠ I. Comparison of mass transfer models for the numerical prediction of sheet cavitation around a hydrofoil [J]. International Journal of Multiphase Flow, 2011, 37(6): 620–626.
- [11] SPALART P R, SHUR M. On the sensitization of turbulence models to rotation and curvature [J]. Aerospace Science and Technology, 1997, 5(1): 297–302.
- [12] CHAHINE G L. Nuclei effects on cavitation inception and noise [C]//Proceedings of the 25th Symposium on Naval Hydrodynamics. St. John's, Newfoundland and Labrador, Canada: [s.n.], 2004.

[Continued on page 30]

